Metastability and Paramagnetism in Superconducting Mesoscopic Disks

J. J. Palacios*

Departamento de Física Teórica de la Materia Condensada, Universidad Autónoma de Madrid, Cantoblanco, Madrid 28049, Spain

(Received 10 August 1999)

A projected order parameter is used to calculate not only local minima of the Ginzburg-Landau energy functional but also saddle points or energy barriers responsible for the metastabilities observed in superconducting mesoscopic disks [A. K. Geim *et al.,* Nature (London) **396**, 144 (1998)]. We calculate the local minima magnetization and find the energetic instability points between vortex configurations with different vorticity. We also find that, for any vorticity, the supercurrent can reverse its flow direction on decreasing the magnetic field before one vortex can escape.

PACS numbers: 74.60.Ec, 74.76.–w

The interest in understanding the creation and annihilation mechanisms and, in general, the stability of vortices in superfluids has been recently boosted by a series of technological advances in both mesoscopic superconductors [1–4] and atomic condensates [5]. Most of the proposals for the creation of vortices in atomic condensates face, at the present time, severe technological difficulties. On the contrary, mesoscopic superconductors in magnetic fields are already proving to be an ideal scenario where the detection and even manipulation of vortices at the individual level are becoming more and more feasible [1–4]. A good example, although not the only one, of single-vortex sensitivity can be found in the Hall magnetometry measurements performed on mesoscopic Al disks by Geim *et al.* [2,3]. Both field-cooled (FC) and constant temperature (CT) magnetization measurements provide evidence of the quantization of the vorticity of the order parameter.

Geim's experiment sheds light on the controversial paramagnetic Meissner effect (PME) confirming that the PME, at least in mesoscopic samples, is linked to a nonequilibrium magnetic response of the system. When the system is kept out of equilibrium, it can show paramagnetic response both in the CT and FC cases, whereas, as expected, equilibrium measurements *always* exhibit diamagnetism. In addition to this, the experiment raises a number of other fundamental questions concerning the properties of few-vortex states in mesoscopic systems: (i) What is the origin of the metastability of a given vortex state? (ii) Why can metastable states exhibit paramagnetism? (iii) What is the nature of the instability that triggers a change in the number of vortices? We anticipate the answers to these questions. (i) The metastability results from the sample surface which favors a large surface superconductivity and opposes both vortex escape and entrance. This translates into a very stable vorticity or topological charge, Q, associated with all the local minima of the energy functional. (ii) On decreasing the magnetic field, a reversal in the direction of the total supercurrent flow associated with most local minima can take place before vortices escape. In general, and in contrast with recent work, detector effects [6] need not be invoked to explain the paramagnetic response. (iii) The ultimate mechanism responsible for an instability in the vorticity or change in the number of vortices of the system is the disappearance of the saddle point separating a local minimum from a neighboring one with different Q. This is called energetic instability. We argue below that, either increasing or decreasing the magnetic field, there seems to be experimental evidence that this energetic instability is preempted by another mechanism, either associated with noise or some other type of fluctuations (thermal or quantum).

We start from the Ginzburg-Landau functional for the Gibbs free energy difference between the normal and superconducting states in an external magnetic field H:

$$G = \int d\mathbf{r}\left[\alpha|\Psi(\mathbf{r})|^2 + \frac{\beta}{2}|\Psi(\mathbf{r})|^4 + \frac{1}{2m^*}\left|\left(-i\hbar\nabla - \frac{e^*}{c}\mathbf{A}(\mathbf{r})\right)\Psi(\mathbf{r})\right|^2 + \frac{[h(\mathbf{r}) - H]^2}{8\pi}\right], \quad (1)$$

where $\Psi(\mathbf{r})$ is the order parameter or Cooper pair wave function, $h(\mathbf{r}) = \nabla \times \mathbf{A}(\mathbf{r})$, and α and β are the condensation and interaction energy parameters, respectively. Numerical minimization procedures have been used in the past [6–8] to find global and even local minima of the Ginzburg-Landau functional applied to mesoscopic superconducting disks. However, saddle points or energy barriers, which are essential for the analysis of the stability of the local minima, cannot be easily obtained from these methods. Before going into the details of how to overcome this problem, a few comments are in order. It is well known that the magnetic response to an external magnetic field of a superconductor varies with its size, geometry, and orientation with respect to the field in a nontrivial way. Type-I superconductors expel the magnetic field below the critical temperature, but, for the largest disks in Geim's experiment, the magnetic field can penetrate the interior [2,3]. Moreover, multiple-vortex structures [7,9], expected only in type-II superconductors, clearly reflect in

 0031-9007/00/84(8)/1796(4)$15.00

the FC measurements [3] (see below). In summary, these disks behave like type-II superconductors, which makes it possible, in a range of fields, to consider a uniform magnetic induction $h(\mathbf{r}) = B$ [9]. Next, we project the order parameter onto the "lowest Landau level" subspace [9,10]:

$$\Psi(\mathbf{r}) = \sum_L C_L \frac{1}{\ell\sqrt{2\pi}} e^{-iL\theta}\Phi_L(r). \qquad (2)$$

This subspace is spanned by normalized eigenfunctions of the linearized differential Ginzburg-Landau equations where L is the angular momentum (≥ 0) and $\Phi_L(r)$ is the associated nodeless function subject to the boundary conditions of zero current through the surface. In this expansion $C_L \equiv |C_L|e^{i\phi_L}$ are complex coefficients and the radial unit is the magnetic length $\ell = \sqrt{e^*\hbar/cB}$. We are considering the thickness of the disk to be smaller than the coherence length so that the system becomes effectively two dimensional. This expansion has been shown to give good qualitative as well as quantitative results for the equilibrium properties at moderately high fields [9].

The central idea in our method for finding generic stationary solutions of the Ginzburg-Landau functional is to project the order parameter onto smaller subspaces spanned by a finite number N of eigenfunctions, $\{L_1, L_2, \ldots, L_N\}$, where $0 \leq L_1 < L_2 < \cdots < L_N$. We will restrict our discussion to a disk radius $R = 5\xi(0)$ which approximately corresponds to the largest disk in Geim's experiment [3] [$\xi(0)$ is the coherence length at $T = 0$]. For such a disk size subspaces with dimension $N > 3$ do not play any role [9] and the projected Ginzburg-Landau functional reduces to

$$G = (B - H)^2 + \sum_{i=1}^{N} \alpha[1 - B\epsilon_{L_i}(B)]|C_{L_i}|^2 + \frac{1}{4}\alpha^2\kappa^2 BR^2\left[\sum_{i=1}^{N} I_{L_i}(B)|C_{L_i}|^4 + \sum_{j>i=1}^{N} 4I_{L_iL_j}(B)|C_{L_i}|^2|C_{L_j}|^2\right] + \ldots, \qquad (3)$$

where the Gibbs free energy is expressed in units of $H_{c2}^2 V/8\pi$ (V being the volume of the disk), $\epsilon_L(B)$ is the energy of the quantum state L expressed in units of $\hbar\omega_c/2$ ($\omega_c = e^*B/m^*c$), R is expressed in units of the coherence length $\xi(T)$, and B and H are given in units of $H_{c2}(T)$. The interactions appear in $I_L(B) \equiv \int dr\, r\Phi_L^4$, which can be interpreted as the interaction between Cooper pairs occupying the same quantum state L, and $I_{L_iL_j}(B) \equiv \int dr\, r\Phi_{L_i}^2\Phi_{L_j}^2$, accounting for the interaction between Cooper pairs occupying different quantum states. Interaction terms that depend on the phases of the coefficients appear when $L_1 + L_3 = 2L_2$ [9], but they are not considered here since these subspaces do not play any role in our discussion. Stationary solutions of the projected functional (3) can thus be found analytically with respect to $|C_L|$ and numerically with respect to B.

As we have anticipated, in the expression (3) κ does not take on the bulk nominal value for Al, but an effective one that takes into account the geometry of the disk. It is very difficult to estimate this effective value, but the experimental evidence of the existence of multiple-vortex structures for the $R = 5\xi(0)$ disk along with recent detailed numerical calculations [7] indicate that $\kappa \gtrsim 1$. We will consider $\kappa = 1$ throughout. The main results of this work are shown in Fig. 1 which shows the magnetization associated with all the energetically stable stationary solutions, i.e., all the local minima. These local minima are characterized by a vorticity or topological charge Q which is defined as the number of times that the phase of the order parameter winds around 2π as we complete one circumference moving along the inner surface of the disk. Different curves correspond to different values of Q. Along any of these curves the topological charge distributes itself in a variety of ways. For large Q ($Q \geq 12$), the local minimum is always a giant vortex with $L = Q$. This local minimum is separated from neighboring local minima with $L = Q + 1$ and $L = Q - 1$ by saddle points which appear as energetically unstable stationary solutions in the subspaces $\{Q, Q + 1\}$ and $\{Q - 1, Q\}$, respectively. Figure 2(b) shows an example of the modulus of the order parameter at the saddle point that separates the giant vortex $L = 9$ from the $L = 10$ close to the high-field end of the $Q = 9$ curve. Notice the strong depletion of the order parameter at an (arbitrary) point on the surface [11]. Higher-energy saddle points also appear separating the giant vortex $L = Q$ from other possible local minima

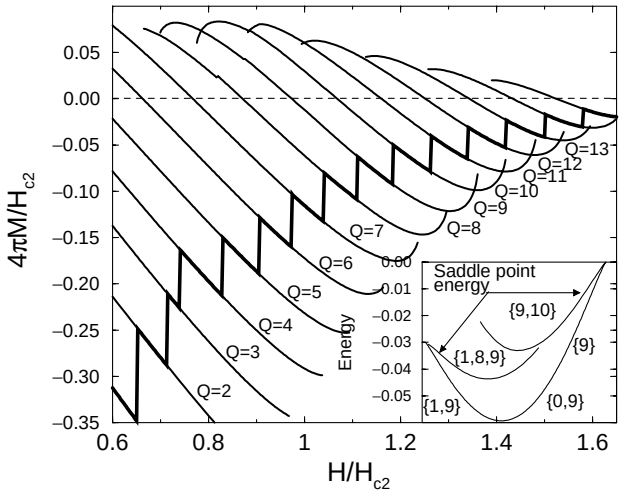

FIG. 1. CT magnetization curves associated with local minima of different topological charges Q for a disk radius $R = 5\xi(0)$ and $\kappa = 1$. The equilibrium magnetization is represented by the thick solid line. Inset: Energy of the local minimum $Q = 9$ compared to the energy of the saddle points that separate it from the closest neighboring local minima.

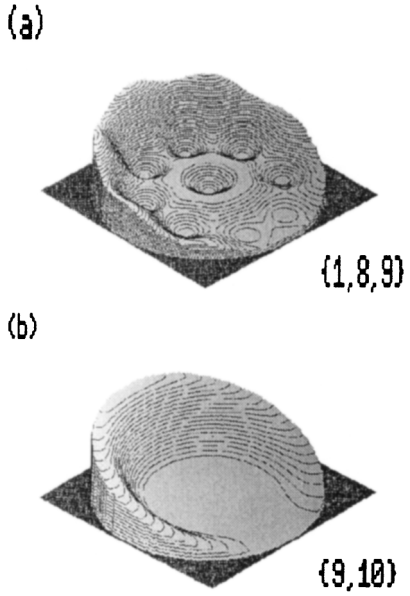

FIG. 2. Modulus of the order parameter at the saddle points separating the local minimum (a) $\{1, 9\}$ from $\{1, 8\}$ close the low-field end of the $Q = 9$ curve and (b) $\{9\}$ from $\{10\}$ close the high-field end of the same curve.

$L = Q + 2$, $L = Q - 2$, etc., which fully guarantees its energetic stability. At the low- and high-field ends of the curve the local minimum $L = Q$ merges with the saddle points $\{Q - 1, Q\}$ and $\{Q, Q + 1\}$, respectively (see, for instance, the high-field side of the inset in Fig. 1). In the presence of dissipation the system will be driven toward the neighboring local minimum. (A dynamical analysis [12] of this process would be interesting, but it is beyond the scope of this work.) For smaller Q ($Q < 12$) a giant vortex can be typically found close to the high-field end of the curve, but, as we move along the curve towards lower values of H, we cross the critical field where the multiple vortex solution in the form of a ring, $\{0, Q\}$, becomes energetically favorable [8,9]. There is no barrier separating them, and a weak second order phase transition takes place. Similarly, there are saddle points separating the solution $\{0, Q\}$ from the local minima $\{0, Q - 1\}$ and $\{0, Q + 1\}$ on neighboring curves. These barriers appear as stationary solutions in the subspaces $\{0, Q - 1, Q\}$ and $\{0, Q, Q + 1\}$, respectively. There is also a barrier separating the local minimum $\{0, Q\}$ from a local minimum $\{1, Q\}$ which may become energetically favorable as we move upwards along the curve. There is a saddle point separating them, which appears as a stationary solution in the subspace $\{0, 1, Q\}$. These saddle points are typically 1 or 2 orders of magnitude smaller than those separating states with different topological charges, although, at the energy crossing, they still range from $\approx$50 K ($Q = 8$) to $\approx$0.1 K ($Q = 11$). The experimental temperature is 0.4 K, which means that the system could evolve along the state $\{0, Q\}$ in the absence of fluctuations. Otherwise, the system would experience a weak first order transition on crossing the barrier and changing the vortex structure into a ring with a vortex in the middle [13]. We have chosen this possibility in our plot, although these first order transitions barely reflect in the magnetization. More structural changes and more weak first order transitions can take place as one moves along the curve on decreasing H. At the low-field end of the curve, the saddle point separating the local minimum $\{L_1, \ldots, Q\}$ from $\{L_1, \ldots, Q - 1\}$, i.e., the $\{L_1, \ldots, Q - 1, Q\}$ stationary solution, merges with the local minimum $\{L_1, \ldots, Q\}$ (see, for instance, the low-field side of the inset in Fig. 1) and the energetic instability sets in. Before reaching the low-field end, as Fig. 2(a) shows, the superconducting density exhibits a strong depletion at some point on the surface when crossing the saddle point.

As Fig. 1 shows, the magnetization associated with the local minima changes sign at some intermediate value of H (which depends on Q). In other words, the supercurrent reverses the direction in which it flows. At this point the height of the vortex escape barrier approaches, typically, its maximum value (see inset of Fig. 1 where the zero-magnetization point coincides with the minimum in the free energy). As already mentioned, these barriers can be several orders of magnitude the experimental temperature. Thus, whatever mechanisms may be operating to decrease the topological charge are unlikely to be efficient enough to prevent the appearance of the paramagnetic response on decreasing H. In fact, this is what is observed in the experiment. The sign change in the response occurs approximately when the dominant eigenfunction in the expansion of the order parameter, $L_N = Q$, crosses the minimum of the band structure $\epsilon_L(B)$ and reverses its group velocity. As was shown in Refs. [9,10], the minimum in the band structure comes about due to the boundary conditions imposed on the components of the order parameter. Notice that detector size effects need not be invoked [6] to account for the paramagnetic response.

The experimental magnetization curves [3] are, to a large extent, similar to the theoretical ones for small Q. However, for large Q, where our method is expected to be more reliable, there are significant discrepancies. The derivative with respect to the field of the magnetization curves changes sign close to the low- and high-field ends of the curves. Furthermore, neighboring curves even get to cross each other. This is never seen in the experiment [3] which seems to indicate that a vortex can escape or enter the disk before the saddle point or barrier disappears. Since thermal activation is efficient only very close to both ends of the curves, either experimental noise or quantum fluctuations may be ultimately responsible for the vorticity change.

Even if the energetic instability on the diamagnetic side is preempted by some of the relaxation processes mentioned above, the magnetization associated with the global minimum (thick line in Fig. 1) is not likely to be observed for increasing field without intentional relaxation. It has been suggested in the literature that surface

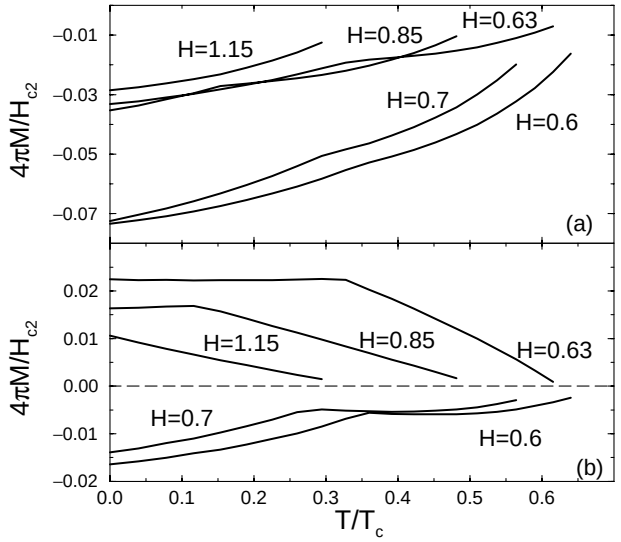

FIG. 3. (a) FC magnetization for a disk of radius $R = 5\xi(0)$ and $\kappa = 1$ at different values of the external magnetic field. Each curve corresponds to the topological charge Q_n of the giant vortex that nucleates at the highest critical temperature. (b) The same as in (a), but for a topological charge $Q_n + 1$.

roughness is responsible for the destruction of the saddle points associated with the surface barrier. The saddle points preventing the escape or entrance of vortices have the same origin, and surface roughness should affect them similarly. Thus, in our view, there are no reasons for the system to follow the ground state on increasing H, and it is expected to continue along a given curve until the onset of the energetic instability or until vortex entrance rates increase to typical measurement times.

Finally, we comment on the FC measurements. The current understanding of the FC results is summarized in a work by Moshchalkov *et al.* [14] which attributes the FC paramagnetic response to a flux-compression phenomenon. Figure 3 shows the magnetization as a function of temperature for different values of the magnetic field. The usual phenomenological temperature scaling of the parameters in the Ginzburg-Landau functional (1) has been considered [14]. Each curve in Fig. 3(a) corresponds to the topological charge Q_n of the giant vortex that nucleates at the highest possible critical temperature for each chosen field. Q_n is maintained along the different curves down to $T = 0$ due to the presence of the energy barriers discussed above which prevent the change of vorticity. The response is always diamagnetic in clear contrast with the FC data. Figure 3(b) shows magnetization curves for a topological charge $Q_n + 1$. Alternating paramagnetic and diamagnetic behaviors are obtained as a function of H and a low-temperature saturation of the paramagnetic response occurs due to explosion of the giant vortex as suggested by Moshchalkov *et al.* [14]. This behavior is in remarkable agreement with the FC data [3] which seem to suggest that either thermal fluctuations close to the critical temperature or surface roughness favor the nucleation of giant vortices with a higher topological charge than that obtained in our calculations [15]. Notice again that, in our approach, the magnetic field is uniform in space which suggests that flux compression [3,14] is not essential as far as the existence of paramagnetism is concerned. Still, the origin of the PME in the FC measurements of Ref. [3] remains an open issue.

In conclusion, we have addressed some fundamental questions posed by the experiment of Geim *et al.* [3]. Saddle points or barriers of the Ginzburg-Landau functional have been found based on a projection technique. This has allowed us to obtain metastable magnetization curves and to gain insight into the controversial paramagnetic response in both FC and CT magnetization measurements.

The author acknowledges enlightening discussions with J. Dukelsky, J. Fernández-Rossier, J. J. García-Ripoll, A. K. Geim, F. Guinea, B. Paredes, G. Sierra, and C. Tejedor. This work has been funded by MEC of Spain under Contract No. PB96-0085.

*Present address: Dept. de Fisica Aplicada, Universidad de Alicante, San Vicente del Raspeig, 03690 Alicante, Spain.

[1] V. V. Moshchalkov *et al.*, Nature (London) **373**, 319 (1995).
[2] A. K. Geim *et al.*, Nature (London) **390**, 259 (1997).
[3] A. K. Geim *et al.*, Nature (London) **396**, 144 (1998).
[4] C. A. Bolle *et al.*, Nature (London) **399**, 43 (1999).
[5] See, for instance, D. A. Butts and D. S. Rokshar, Nature (London) **397**, 327 (1999), and references therein.
[6] P. S. Deo, V. A. Schweigert, and F. M. Peeters, Phys. Rev. B **59**, 6039 (1999).
[7] V. A. Schweigert, F. M. Peeters, and P. S. Deo, Phys. Rev. Lett. **81**, 2783 (1998).
[8] P. S. Deo, V. A. Schweigert, F. M. Peeters, and A. K. Geim, Phys. Rev. Lett. **79**, 4653 (1997); V. A. Schweigert and F. M. Peeters, Phys. Rev. B **57**, 13 817 (1998).
[9] J. J. Palacios, Phys. Rev. B **58**, 5948 (1998); Physica (Amsterdam) **256–258B**, 610 (1998).
[10] J. J. Palacios, Phys. Rev. B **57**, 10 873 (1998).
[11] For a detailed analysis of this depletion phenomenon see V. A. Schweigert and F. M. Peeters, Phys. Rev. Lett. **83**, 2409 (1999).
[12] I. Aranson, B. Ya. Shapiro, and V. Vinokur, Phys. Rev. Lett. **76**, 142 (1996).
[13] A. K. Geim, S. V. Dubonos, and J. J. Palacios (unpublished).
[14] V. V. Moshchalkov, X. G. Qiu, and V. Bruyndoncx, Phys. Rev. B **55**, 11 793 (1997).
[15] Similar conclusions were reached in Ref. [14] using a numerical method that considers a nonuniform magnetic induction $b(r)$. The authors, however, attributed the discrepancy between theory and experiment to numerical uncertainty in their calculations.